6 THREE-DIMENSIONAL SPATIAL DISTRIBUTION OF SCATTERERS IN GALERAS VOLCANO, SOUTH-WESTERN COLOMBIA

6.1 INTRODUCTION

In this chapter we will focus on the imaging of small-scale heterogeneities by the estimation of three-dimensional spatial distribution of relative scattering coefficients from shallow earthquakes occurred under the Galeras volcano region. The technique for the inversion of coda-wave envelopes was previously developed in Chapters 3 and 4. In this case, among the possible inversion methods to use for solving the problem, we will use the Filtered Backprojection method, because in Chapter 5 it was demonstrated that the results were almost independent of the inversion method used. Moreover, the FBP method required much less computation time to perform the inversion.

Galeras is a 4276-m high andesitic stratovolcano in south-western Colombia near the border to Ecuador (see Figure 6-1). It is a 4,500 years old active cone of a more than 1 Ma old volcanic complex located in the Central Cordillera of the south-western Colombian Andes. It is historically the most active volcano in Colombia and it has been reactivated frequently in historic times [65]. It awakened again gradually in 1988 after more than 40 years of repose.

Galeras is situated at 1°14'N and 77°'22'W, and its active summit raises 150 m up from the 80 m deep and 320 m wide caldera, which is open to the west (see Figure 6-2). The present active crater lies about 6 km west of Pasto, which has a population of more than 300,000 and with another 100,000 people living around the volcano. Although it has a short-term history of relatively small-to-moderate scale eruptions, the volcanic complex has produced major and hazardous eruptions [Calvache et al. [66], 1997] thus constituting a potential risk to the human settlements in this region.

There are also three smaller craters in the caldera. The diameter on the foot of

the volcano is 20 kilometres. Long term extensive hydrothermal alteration has affected the volcano. This has contributed to large-scale edifice collapse that has occurred on at least three occasions, producing debris avalanches that swept to the west and left a large horseshoe-shaped caldera, inside which the modern cone has been constructed. Major explosive eruptions since the mid Holocene have produced widespread tephra deposits and pyroclastic flows that have swept down all but the southern flanks.

Galeras was designated a Decade Volcano in 1991, which identified it as a target for intensive and interdisciplinary study during the United Nations' International Decade for Natural Disaster Reduction. With the aim of enlarging the knowledge of the internal structure of the volcano as well as to serve for its seismic hazard assessment, the present study is a different complementary contribution to the interdisciplinary research (geological, geophysical and geochemical) being conducted in the region since the re-activation of Galeras volcano.
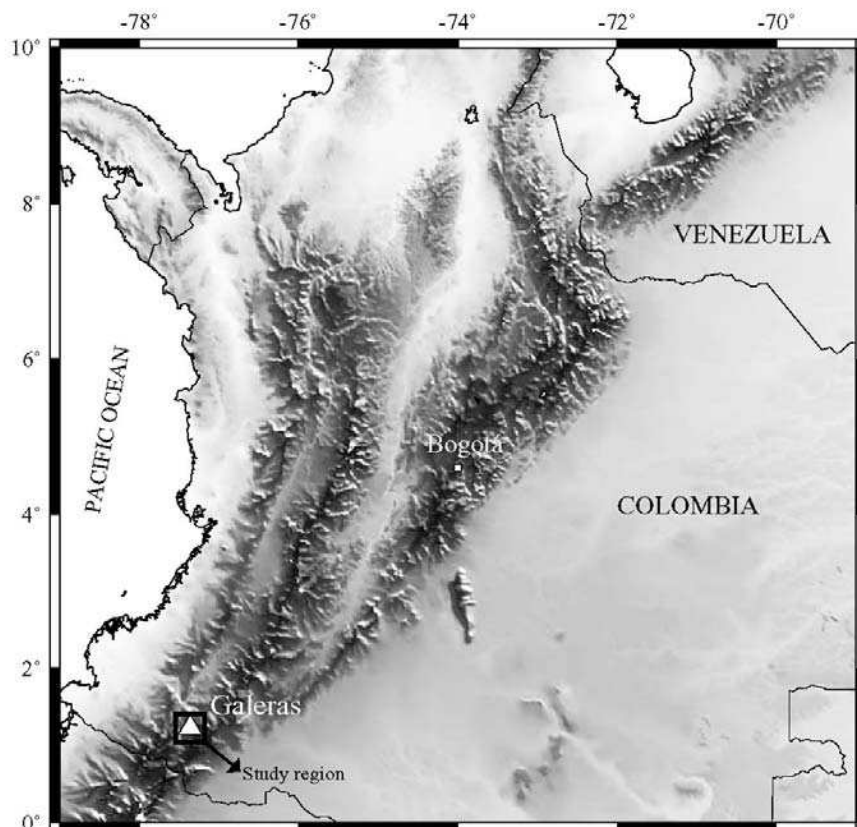

Figure 6-1. Topographic map of Colombia showing the location of the Galeras volcano and the study area.

6.2 GEOLOGICAL SETTING

6.2.1 GEOLOGICAL HISTORY

Galeras has been erupting lavas and pyroclastic flows during the last million years. Two major caldera-forming eruptions have occurred, the first about 560,000 years ago in an eruption which expelled about 15 cubic kilometres of material, and the second some time between 40,000 and 150,000 years ago, in a smaller but still sizable eruption of 2 km³ of material. Subsequently, part of the caldera wall has collapsed, probably due to instabilities caused by hydrothermal activity, and later eruptions have built up a smaller cone inside the now horseshoe-shaped caldera.

Figure 6-2. Galeras volcano from the west flank. Photo by Norm Banks of USGS [67].

At least six large eruptions have occurred in the last 5000 years, most recently in 1886, and there have been at least 20 small to medium sized eruptions since the 1500s.

Galeras is one of the 16 Decade Volcanoes identified by the International Association of Volcanology and Chemistry of the Earth's Interior (IAVCEI) as being worthy of particular study in light of their history of large, destructive eruptions and proximity to populated areas. The Decade Volcanoes project encourages studies and

public-awareness activities at these volcanoes, with the aim of achieving a better understanding of the volcanoes and the dangers they present, and thus being able to reduce the severity of natural disasters. The project was initiated as part of the United Nations-sponsored International Decade for Natural Disaster Reduction.

Galeras had become active in 1988 after 40 years of dormancy. In 1993, the volcano erupted when several volcanologists were inside the crater taking measurements. The scientists had been visiting Pasto for a conference related to the volcano's designation as a Decade Volcano. Six were killed, together with three tourists on the rim of the crater. The eruptive period lasted until 1995. Since then, the volcano has been in a relative calm stage with some ash and gas emission episodes and low-level eruptive activity (a crater located to the east of the main one was re-activated in 2002 after more than 10 years of inactivity) dusting nearby villages and towns with ash. A new eruptive episode began in 2004 (three explosive events have occurred in this period) and it continues active at the time of this writing (the activity reports are available at http://www.volcano.si.edu/).

The volcano has continued to be well studied, and the studies concerning predictions of eruptions at the volcano have improved. One phenomenon which seems to be a reliable precursor to eruptive activity is a shallow-source, low frequency seismic events known as a "tornillos" which are related to magmatic activity and that have also been recorded during different stages of volcanic activity at Galeras [Gómez and Torres, 1997 [68]]. These have occurred before about four-fifths of the explosions at Galeras, and the number of "tornillo" events recorded before an eruption is also correlated with the size of the ensuing eruption.

Seismicity in the region since 1988 has been characterized by long period events, volcano-tectonic earthquakes and tremor episodes. The level of seismic activity has presented fluctuations, alternating periods of low-level seismicity with episodes of seismic activity increase in terms of the number and/or magnitude of the events. Some shallow (up to 8 km) volcano-tectonic earthquakes have reached local magnitudes up to 4.7.

6.2.2 GEOLOGY OF GALERAS VOLCANO

Galeras is located in a region with a metamorphic rock basement of Precambrian and Paleozoic ages [69]. The basement is overlaid by metamorphic rocks of Cretacic age with low and medium grade associated with amigdular metabasalts. All of this is covered by volcano sedimentary units of Tertiary age that made a plateau, over which the Pleistocenic and Holocenic volcanoes have emerged. The tectonic plate of this region is very complex, as a result of the collision between the Nazca and south American plates. This causes the uplift of the Andes and the volcanism in the region. The structural trend is N40°E and the principal tectonic feature is the Romeral Fault Zone, which has been interpreted as the limit between continental crust to the east and the oceanic crust to the west (Barrero, 1979). This system includes the Silvia-Pijao and Buesaco faults, both of which cross under Galeras, and are associated with many old caldera systems as can be seen in Figure 6-3.
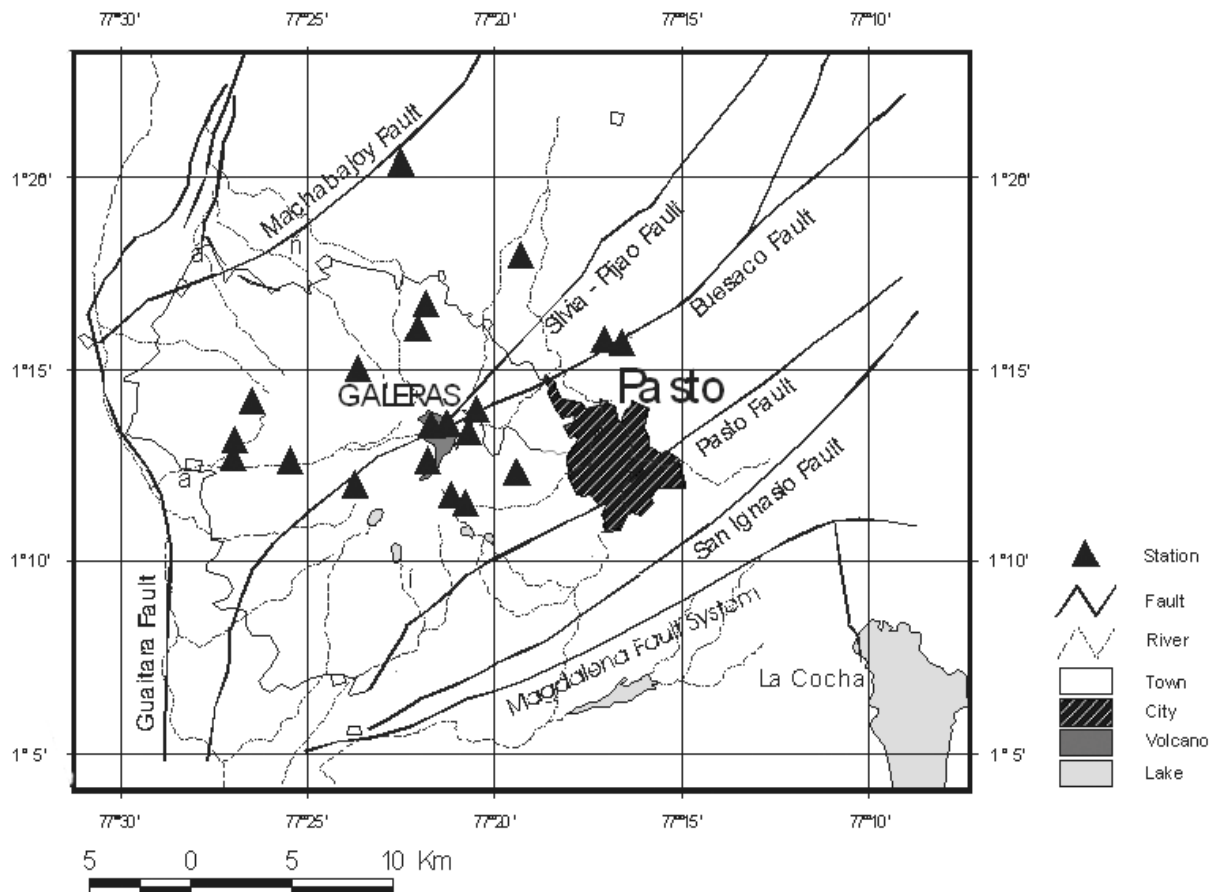

Figure 6-3. Geological map of the Galeras Region. The map includes the locations of the stations.

Galeras is a stratovolcano. Stratovolcanos are usually tall, conical mountains composed of both hardened lava and volcanic ash. The shape is characteristically steep in profile because lava flows that formed them were highly viscous, and so cooled and hardened before spreading very far. Such lava tends to be high in silica (mafic magma). All these characteristics apply to the Galeras volcano. In Figure 6-4 altitude curves are represented and the shape and steepness of this volcano becomes evident. Stratovolcanoes are often created by subduction of tectonic plates as in our case.
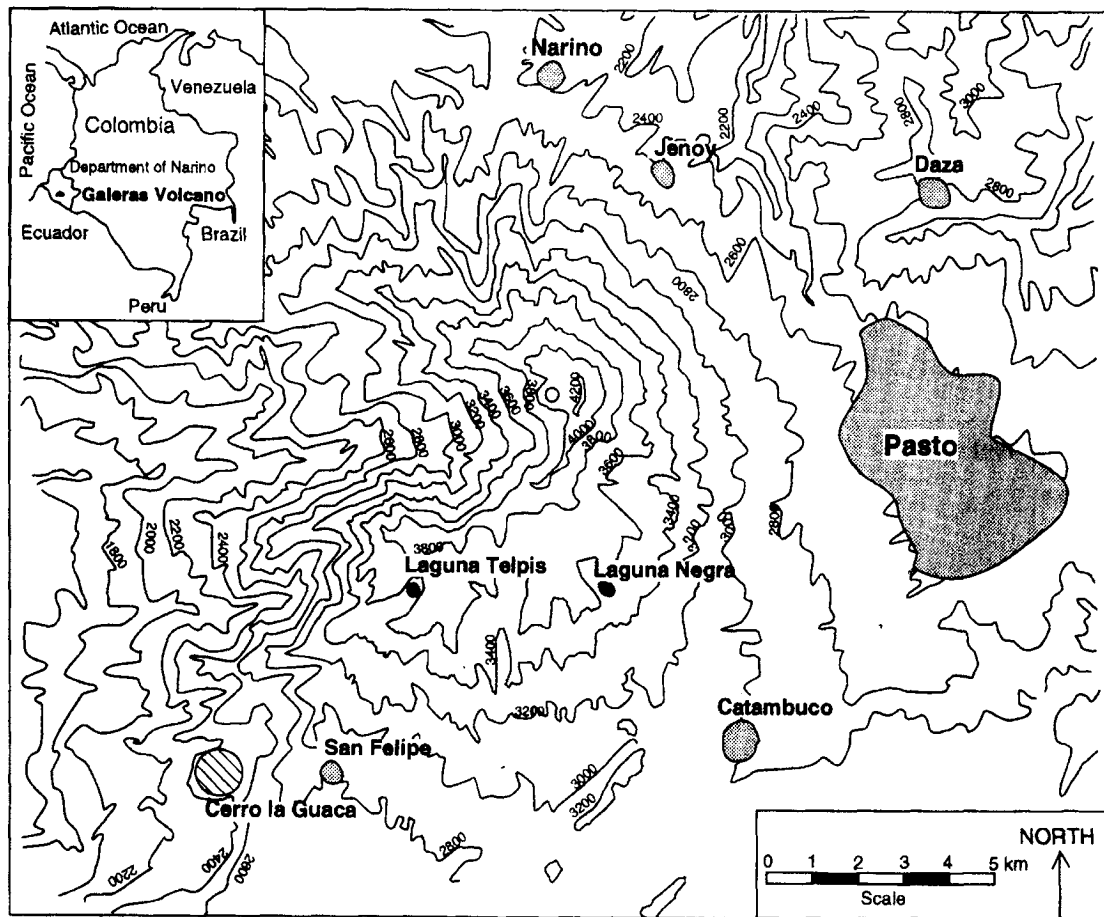

Figure 6-4. Map showing the shape of Galeras volcano and altitude curves [72].

Studying SO_2 emissions it is possible to infer the internal structure of the Galeras volcano. The emissions of SO_2 are not constant. Usually, emissions decrease with time. Then, during eruption periods, emissions become intense. When the eruption has finished, a new period of emission decrease starts over again. The general decrease of the flux with time is interpreted as a progressive degassing of a single batch of magma followed by the obstruction of the conduit by emplacement of the dome. The

large amounts of sulfur degassed from Galeras strongly suggest that a reservoir of sulphur rich magma underlies the shallow magma in the conduit of the active cone.
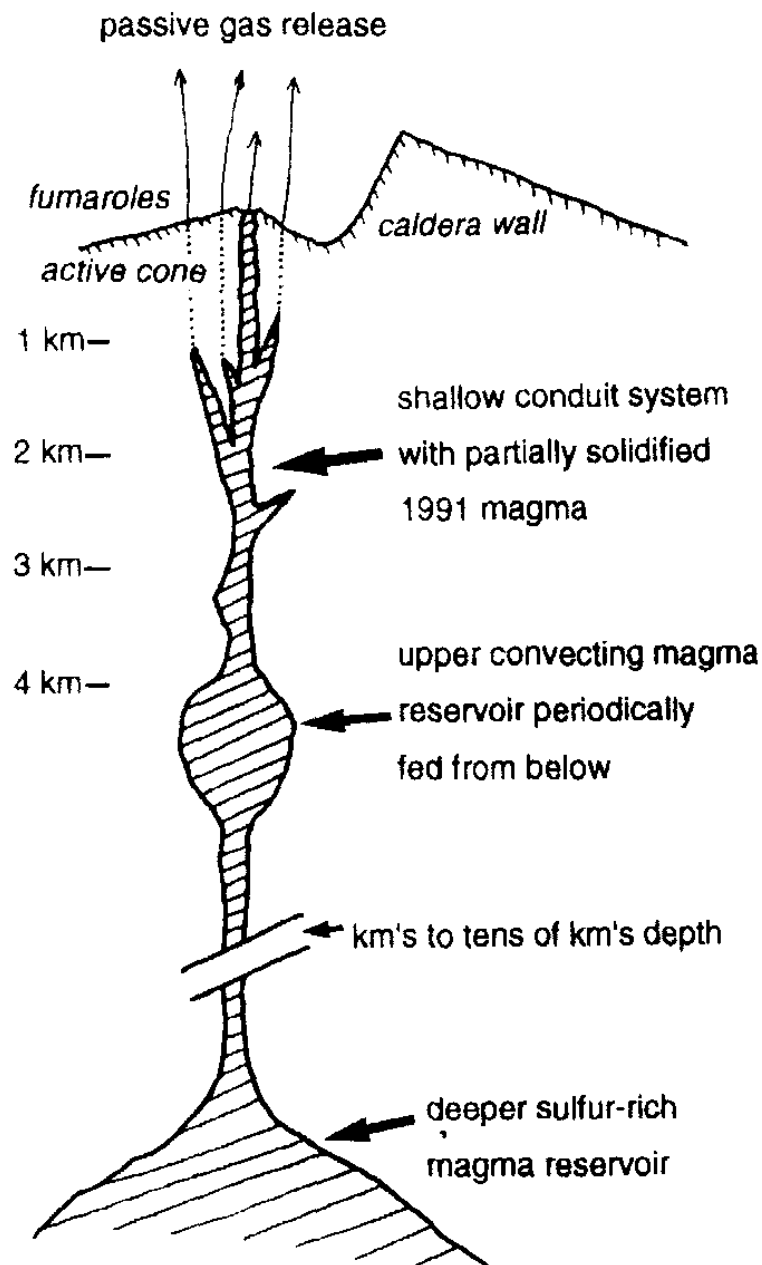

Figure 6-5. Sketch of the magmatic plumbing system beneath Galeras [72].

The presence of this hypothetical reservoir is also supported by petrologic and seismic data [70] which indicate that the reservoir is located at a depth of 4-5 km, The reservoir is able to supply SO_2 and other gasses to the upper, more open and fractured

reaches of the volcano through a complex conduit system. Strong degassing fumaroles are surface expressions of this upper conduit system. As the reservoir cools becomes less convective and the result is a progressive decline in SO_2 fluxes from the volcano. Then, the reservoir becomes isolated: the reservoir is no longer feed with fresh magma from deeper regions. During a reactivation cycle, the reservoir is initially supplied with mafic, sulphur rich magma from a deeper level after a repose period of tens of years. This supply of magma could be the result of tectonic disturbances nearby. Once this occurs, the magma can degas from the upper reservoir through the shallow conduit system and eventually rise to erupt explosively or effusively.

Then, the behaviour suggests that the internal structure of the Galeras volcano is like the one outlined in Figure 6-5, where the magmatic plumbing system beneath Galeras is sketched. The plumbing system comprises the following structures:

i) A sulphur-rich mafic magma at intermediate to deep levels in the crust

ii) An upper reservoir fed from deeper levels

iii) Shallow conduits through which most of the degassing takes place

6.3 DATA DESCRIPTION

Data used in this study is a selection of 1564 high quality coda waves' recordings from shallow earthquakes (depths less than 10 km from the Earth's surface) with local magnitudes less than 2.0 occurred in the region since 1989 to 2002. The 31 short-period (T_0=1 s), vertical component recording stations used were deployed at different stages of the Galeras seismic network operation and they were located at distances less than 10 km from the active crater. The three-dimensional distribution of hypocenter and stations can be seen in Figure 6-6 and the coordinates and designation of each station can be found in Table 6-1.
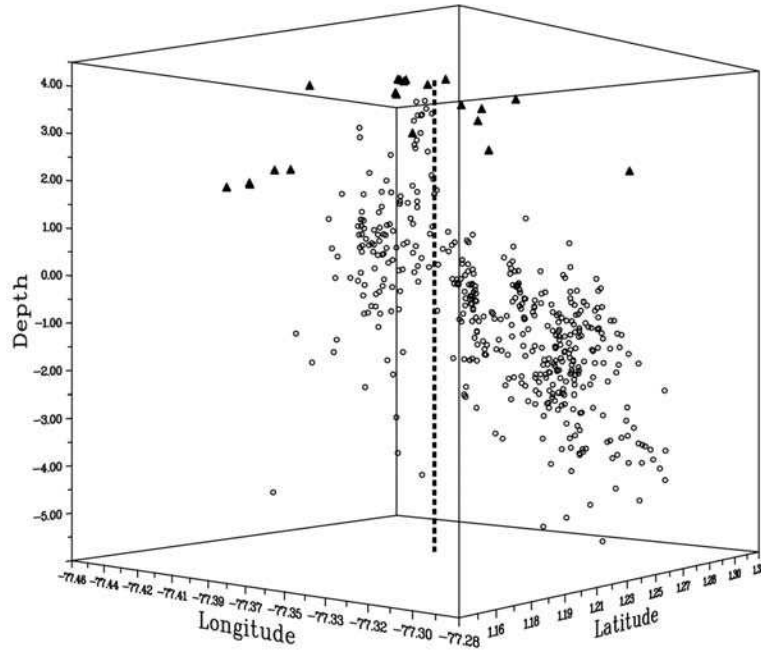
Figure 6-6. Three-dimensional of hypocenters (green circles) and stations (blue triangles).

Station number	Name	Latitude (º)	Longitude (º)	Altitude (km)
0	ARLS	1.2500	-77.3913	3250
1	CALA	1.2063	-77.4227	2353
2	CB2R	1.1910	-77.3490	3625
3	CB3D	1.1910	77.3490	3625
4	COB3	1.1910	77.3490	3625
5	CON4	1.2053	-77.4478	2050
6	COND	1.1938	-77.3925	4000
7	CONO	1.2202	-77.3588	4010

Station number	Name	Latitude (º)	Longitude (º)	Altitude (km)
8	CR2D	1.2102	-77.3607	4058
9	CR2G	1.2107	-77.3620	4032
10	CR2R	1.2773	-77.3620	4032
11	LOEW	1.3537	-77.3780	2350
12	LOMV	1.3537	-77.3780	2350
13	LONS	1.3537	-77.3780	2350
14	NAR2	1.2688	77.3687	2870
15	OLGA	1.2223	-77.3523	4100
16	PLAZ	1.2593	-77.2790	3000
17	PUYI	1.2977	-77.3230	2370
18	TEL2	1.257700	-77.2740	3070
19	URCR	1.2188	-77.3423	3494
20	UREW	1.2188	-77.3423	3494
21	URNS	1.2188	-77.3423	3494
22	CBA2	1.1885	-77.3463	3570
23	CO2R	1.2153	-77.4455	2168

Station number	Name	Latitude (º)	Longitude (º)	Altitude (km)
24	CON2	1.2160	-77.4460	2140
25	CON3	1.2337	-77.4410	2530
26	CRA2	1.2078	-77.3612	4040
27	CRA3	1.2065	-77.3612	4040
28	OBEW	1.2033	-77.3227	3010
29	OBNS	1.2033	-77.3227	3010
30	URCO	1.2260	-77.3387	3435

Table 6-1. Number, name and coordinates of each seismic station from which data has been used**.**

6.4 DATA ANALYSIS

In order to estimate the inhomogeneous spatial distribution of relative scattering coefficients in the crust we followed the method proposed in Chapter 3. The system of equations relating the spatial distribution of relative scattering strength to the observed coda energy residuals under the assumption of single isotropic scattering and spherical radiation of a seismic source can be written as:

$$w_{11}\alpha_1 + \cdots + w_{i1}\alpha_i + \cdots + w_{N1}\alpha_N = e_1$$
$$\vdots$$
$$w_{1j}\alpha_1 + \cdots + w_{ij}\alpha_i + \cdots + w_{Nj}\alpha_N = e_j \qquad (6.1)$$
$$\vdots$$
$$w_{1M}\alpha_1 + \cdots + w_{iM}\alpha_i + \cdots + w_{NM}\alpha_N = e_M$$

We remind that this system of equations is obtained by dividing the coda of each seismogram into several small time windows. Then, in Eq.(6.1) there is an equation for every time window of every seismogram. Also for each time window, the scatterers

contributing to the energy density are contained in a spheroidal shell. Therefore, M is the total number of equations (number of seismograms multiplied by the number of coda time windows considered), and N is the total number of scatterers (number of small blocks into which the study region is divided). The right side of equation (6.1) is called coda wave energy residual (e_j) which measures the ratio of the observed energy density in this part of the coda to the average energy density of the medium.

We will carry out the inversion of the system by using the Filtered Backprojection Algorithm developed in Section 4.5.

Because each analyzed frequency band is giving us information about inhomogeneous structures with sizes comparable to the seismic wavelengths, and given that the signal energy contents of the available data decays abruptly for frequencies f above 12 Hz, we decided to calculate the coda wave energy residuals [Nishigami, 1991 [40]; Ugalde et al., 2005 [71] for the frequency bands 4-8 (6±2) Hz and 8-12 (10±2) Hz, thus allowing us to image structures of sizes comparable to wavelengths of ~400 to ~800 m for 4-8 Hz, and ~300 m to ~400 m for 8-12 Hz. These sizes are derived by considering an average S-wave velocity of β=3.3 km/s in the study region. From the bandpass-filtered seismograms, we calculated the rms amplitudes $A_{obs}(f \mid r,t)$ for each hypocentral distance r by using a 0.25 s spaced moving time window of length $t\pm1$ s, and $t\pm0.5$ s for the 6 Hz and 10 Hz centre frequencies, respectively.

The time interval for the analysis started at 1.5 times the S-wave travel times (in order to increase the resolution near the source region) and had a maximum length of 20 s (to minimize the effects of multiple scattering). We also computed the rms amplitudes for a noise window of 10 s before the P-wave arrival and only the amplitudes greater than two times the signal to noise ratio were kept. Then, the average decay curve was estimated for each seismogram by means of a least-squares regression of $\ln\left[t^2 A_{obs}(f \mid r,t)\right]$ vs. t, where the term t^2 is a geometrical spreading correction which is valid for body waves in a uniform medium. We only kept the estimates with a correlation coefficient greater than 0.60. The observed coda energy residuals $e(t)$ were then calculated by taking the ratio of the corrected observed amplitudes to the estimated exponential decay curve. Finally the residuals were averaged in time windows of

δt =0.25 s to get e_j at discrete lapse times t_j.

A 20 km x 20 km in horizontal and 50 km in depth study region was selected taking into account the stations and hypocenters distribution. It was divided into *N*=50 x 50 x 50 blocks, the volume of which satisfies the condition $\delta t \leq 2(\delta V)^{1/3} / \beta$. Then, the observational system of equations (6.1) was created by assuming the layered velocity structure shown in Table 6-2 and it was solved using the FBP algorithm [Ugalde et al., 2005, [71]].

Depth (km)	S-wave velocity (km/s)
4	2.0
2	2.1
0	2.2
-4	3.4
-22	3.8
-40	4.5

Table 6-2. S-wave velocity model for the Galeras Volcano region**.**

6.5 RESULTS

To check for sampling insufficiencies, we plotted in Figure 6-7 a vertical cross section of the hit counts, or number of coda residuals contributed by each block. The figure shows that the entire region is sampled by the ellipses although the number of hit counts is smaller at the deepest levels and also inside a shallow area to the north-east of the volcano summit.
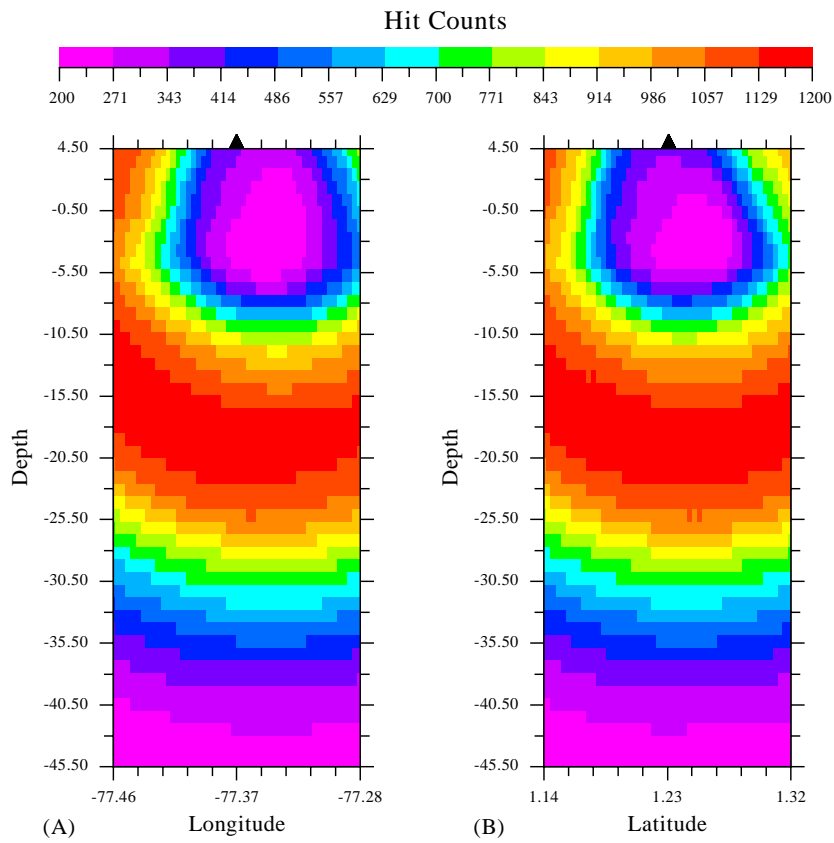
Figure 6-7. Vertical cross sections of the hit count distribution along the parallel 1.23°N (A) and the meridian 77.36°W (B) which correspond to the coordinates of the summit. The Galeras volcano location is indicated by the solid triangle.

The resulting distribution of relative scattering coefficients $\alpha - 1$ in the study region for the analyzed frequency bands and for different depths up to 10 km from the summit is plotted in Figure 6-8. The colour scale indicates the perturbation of scattering coefficients from the average in this region, being the largest values ~3.0 and the minimum ~0.5.
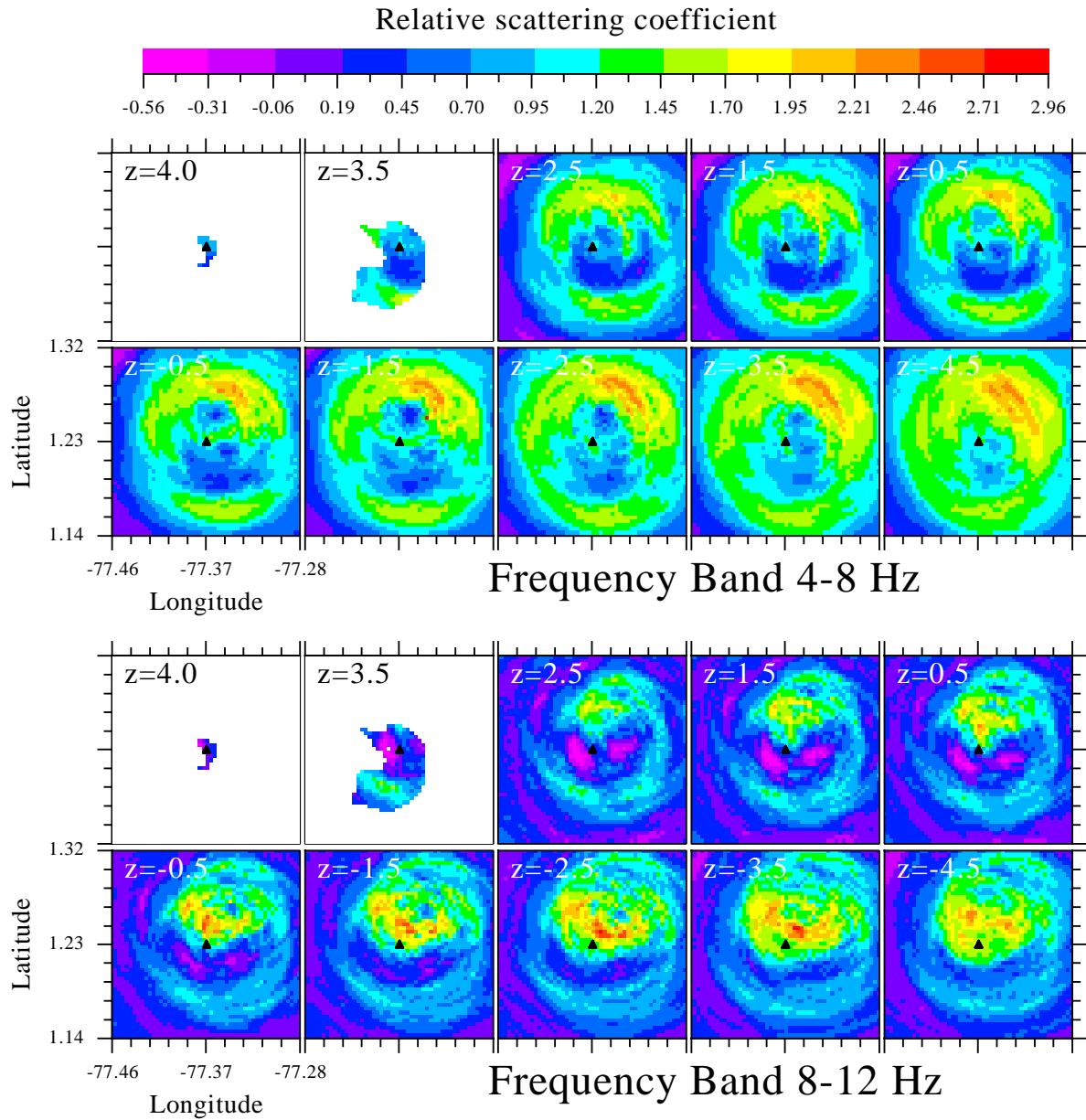
Figure 6-8. Horizontal sections of the study area showing the distribution of the relative scattering strength (α-1) at different depths from 4 km to -4.5 km. The solid triangle indicates the location of the Galeras volcano summit. The topographic contour lines at 4000 m and 3500 m levels are also plotted.

6.6 DISCUSSION

Figure 6-8 shows that the region of ±10 km in horizontal and 10 km in depth centred at the Galeras volcano summit presents a remarkable inhomogeneous distribution of relative scattering coefficients. More than the 83% and the 50% of the analyzed region for low and high frequencies, respectively, reveal a spatial perturbation of the scattering coefficient greater than +50%. For low frequencies, a strong scattering donut-shaped area with relative scattering coefficients between 0.96 and 3.0 is found around the volcano at all depths. The volume showing the strongest relative scattering coefficients (α-1~2.0-3.0) is located to the northeast of the volcano at depths between -0.5 km and -4.5Km. At high frequencies, the strong scattering zone occurs slightly to the north of the axis of the volcano at the same depths. Also we may notice that the scattering strength is similar but slightly lower for the lower frequency band. Then, we may conclude that, at shallow depths, there is a single complex structure located at the north of the volcano that shows a frequency dependent behaviour. The relative scattering coefficients at high frequencies are stronger than those of low frequencies in a volume near the axis of the volcano, which means that small-size heterogeneities as small fractures (comparable to a wavelength of ~300 m to ~400 m for a centre frequency of 10 Hz) contribute more scattered energy than those with larger sizes. On the contrary, heterogeneities with sizes comparable to a wavelength of ~400 to ~800 m for a centre frequency of 6 Hz contribute more to the scattering energy at the north-east of the summit.

Figure 6-9 shows a vertical cross section of the region along the east-west and north-south directions centred at the volcano which shows the scattering perturbation at higher depths. A second strong scattering volume at depths between -29 km and -36 km is clearly observed at high frequencies and can be noticed at low frequencies. Unfortunately, in this case it is more difficult to establish the geometry of the scattering region. The ellipsoidal pattern imaged results from both a poor sampling and the geometry of the ellipses at these deeper levels, which are almost parallel. This makes it possible to establish only the depth and height of the region. A frequency dependence of the strength of the scattering coefficient is again observed thus indicating that small-scale heterogeneities contribute more scattering energy at these deeper levels.
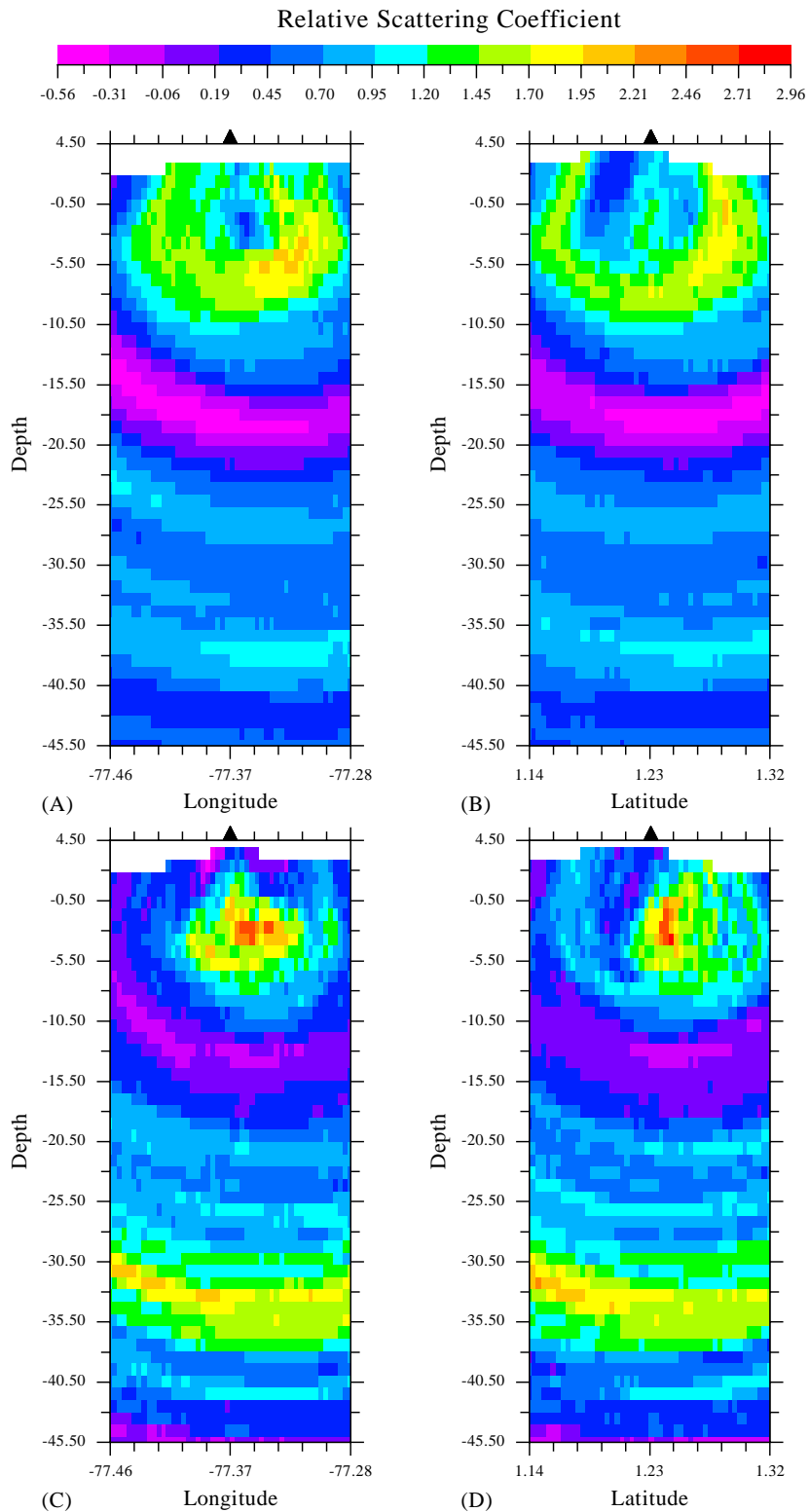
Figure 6-9. Vertical cross section of the study region along the two planes defined by the summit coordinates, which indicated by the solid triangle (latitude 1.23° and longitude -77.36°). The color scale indicates the perturbation of the scattering coefficient α-1 for the 4-8 Hz (A, B) and 8-12 Hz (C, D) frequency bands.

The existence of both structures is in close agreement with the current magmatic plumbing system model beneath Galeras volcano. This model is based on petrologic and seismic data and it proposes a shallow conduit system with a distinct reservoir at a depth of 4-5 km from the summit which is periodically fed from a deeper magma reservoir which is located from km's to tens of km's depth [Calvache, 1990 [70]; Zapata et al., 1997,[72]].
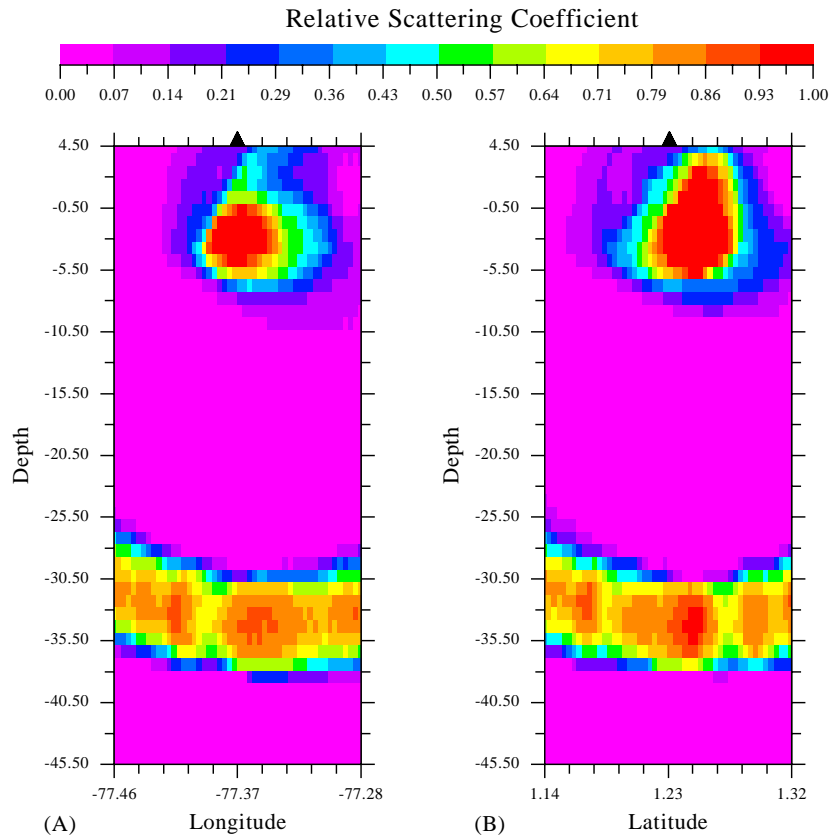

Figure 6-10. Vertical cross section showing the results of the inversion analysis for a synthetic test consisting of two spherical structures buried at depths of -2 km and -33 km.

In order to establish the validity of the results of this study and to help their geological interpretation, we tested the inversion method by means of a synthetic test. We simulated the presence of two magmatic chambers located at the north of the volcano at depths of -2 km and -33 km by two spherical structures with positive perturbations of the scattering coefficient embedded in a non perturbed medium. Then, we synthesized the coda energy residuals from the observational equation using the synthetic pattern of scattering coefficients and the same distribution of stations and

events used in the analysis. Figure 6-10 shows the inversion of the synthesized residuals. It can be observed that both the pattern and the perturbation value of the scattering coefficient were well resolved in the considered region for shallow depths. A comparison of Figure 6-9 and Figure 6-10 suggests a reasonable agreement between synthetic and experimental results, thus supporting the identification of the scattering structures imaged with the magmatic chambers of the geological model.

6.7 CONCLUSIONS

The three-dimensional spatial distribution of relative scattering coefficients has been estimated for the Galeras volcano, Colombia, by means of inversion analysis of coda wave envelopes from 1564 high quality seismic recordings by 31 stations of the Galeras seismograph network. Results reveal a highly non-uniform distribution of relative scattering coefficients in the region for the two analyzed frequency bands (4-8 and 8-12 Hz). Strong scatterers showed frequency dependence, which was interpreted in terms of the scale of the heterogeneities producing scattering. Two zones of strong scattering are detected: the shallower one is located at a depth from 4 km to 8 km under the summit whereas the deeper one is imaged at a depth of ~37 km from the Earth's surface. Both zones may be correlated with the magmatic plumbing system beneath Galeras volcano. The second strong scattering zone may be probably related to the deeper magma reservoir that feeds the system.